molecular pharmaceutics

Article

pubs.acs.org/molecularpharmaceutics

In Vivo Performance of a Novel Fluorinated Magnetic Resonance Imaging Agent for Functional Analysis of Bile Acid Transport

Diana Vivian,[†] Kunrong Cheng,[‡] Sandeep Khurana,[‡] Su Xu,[§] Edwin H. Kriel,[∥] Paul A. Dawson,[⊥,#] Jean-Pierre Raufman,*[,‡] and James E. Polli*[,†]

[†]Department of Pharmaceutical Sciences, University of Maryland School of Pharmacy, Baltimore, Maryland 21230, United States

[‡]Department of Medicine, [§]Department of Diagnostic Radiology and Nuclear Medicine, and [∥]Department of Pathology, University of Maryland School of Medicine, Baltimore, Maryland 21230, United States

[⊥]Department of Internal Medicine, Wake Forest School of Medicine, Winston-Salem, North Carolina 27157, United States

Supporting Information

ABSTRACT: A novel trifluorinated cholic acid derivative, CA-lys-TFA, was designed and synthesized for use as a tool to measure bile acid transport noninvasively using magnetic resonance imaging (MRI). In the present study, the *in vivo* performance of CA-lys-TFA for measuring bile acid transport by MRI was investigated in mice. Gallbladder CA-lys-TFA content was quantified using MRI and liquid chromatography/tandem mass spectrometry. Results in wild-type (WT) C57BL/6J mice were compared to those in mice lacking expression of Asbt, the ileal bile acid transporter. ^{19}F signals emanating from the gallbladders of WT mice 7 h after oral gavage with 150 mg/kg CA-lys-TFA were reproducibly detected by MRI. Asbt-deficient mice administered the same dose had undetectable ^{19}F signals by MRI, and gallbladder bile CA-lys-TFA levels were 30-fold lower compared to WT animals. To our knowledge, this represents the first report of *in vivo* imaging of an orally absorbed drug using ^{19}F MRI. Fluorinated bile acid analogues have potential as tools to measure and detect abnormal bile acid transport by MRI.

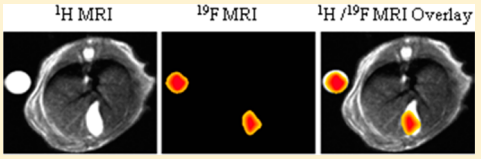

KEYWORDS: *Bile acid transport, fluorine MRI, bile acid malabsorption, enterohepatic circulation*

INTRODUCTION

Together with their classical function as detergents facilitating fat absorption, bile acids have emerged as signaling molecules targeting multiple organs in addition to those associated with their synthesis and enterohepatic cycling.[1,2] Bile acids are synthesized in the liver, stored in the gallbladder, and released into the gut with eating. Although passive absorption occurs throughout the gut, the ileal apical sodium-dependent bile acid transporter (ASBT, encoded by *SLC10A2*) is a key mediator accounting for ∼95% of intestinal bile acid uptake. In Asbt-deficient (*Slc10a2*$^{-/-}$) mice, bile acid absorption is severely impaired, the bile acid pool size is reduced, and excretion of bile acids into the feces is increased.[3]

Bile acid composition and distribution in anatomical compartments are tightly regulated but can be modulated by factors that alter hepatic synthesis and intestinal uptake (e.g., diet, surgery, antibiotic use, and changes in gut flora). Clinical manifestations of bile acid malabsorption (BAM), particularly chronic diarrhea, are thought to result from excess passage of bile acids into the colon due to inadequate absorption in the small intestine. Emerging literature indicates that BAM is underdiagnosed or, more commonly, misdiagnosed as diarrhea-predominant irritable bowel syndrome (IBS); it is estimated that 30−50% of persons with unexplained chronic diarrhea have BAM.[4−7] BAM may result from identifiable causes such as ileal resection, radiation injury, Crohn's disease, or rare dysfunctional mutations in the ASBT gene,[8,9] but in most cases the cause of BAM is not readily apparent. Recently, it has been suggested that BAM may result from overproduction of bile acids in the liver as a consequence of reduced ileal expression and release of fibroblast growth factor (FGF)-19, a physiological feedback inhibitor of bile acid synthesis.[10] In this setting unrestricted hepatic synthesis raises intestinal bile acid concentrations to levels exceeding ASBT transport capacity, thus increasing fecal bile acid levels.

Current approaches to diagnose BAM are limited.[11] Although native and radiolabeled fecal bile acid concentrations can be measured,[12] such assays are time-consuming, not readily available, and expensive. In selected European countries, a ^{75}Se-labeled synthetic bile acid, ^{75}Se-HCAT, is available to measure bile acid transport *in vivo* using a gamma camera.[13] ^{75}Se-HCAT testing, which emits low levels of ionizing radiation, is not approved for clinical use in the United States, where BAM is most commonly diagnosed by evaluating the response to a therapeutic trial of bile acid sequestrants.[11,14] However, bile acid sequestrants, which are not approved for this use by the U.S. Food and Drug Administration, are generally unpalatable, reduce bioavailability of coadministered medicines, and require varying doses across patients. Moreover, diagnosis of BAM

Received: December 11, 2013
Revised: April 3, 2014
Accepted: April 7, 2014
Published: April 7, 2014

using a therapeutic trial of bile acid sequestrants is reported to have a high false-negative rate.[7] Measuring serum levels of FGF-19 or 7-α-hydroxy-4-cholesten-3-one (C4), a byproduct of hepatic bile acid synthesis, has been proposed to diagnose BAM, but these assays require additional clinical validation and are not readily available.[11]

Collectively, these considerations identify the need for innovative approaches to assess bile acid transport *in vivo*. To address this need we sought to develop an accurate, safe, noninvasive, reproducible method of diagnosing abnormal bile acid disposition or transport without the use of ionizing radiation. With the goal of assessing bile acid transport *in vivo* using ^{19}F magnetic resonance imaging (MRI), we synthesized a trifluorinated cholic acid derivative, CA-lys-TFA.[15] ^{19}F is the naturally occurring stable isotope of fluorine and does not suffer from major limitations associated with use of the positron emission tomography (PET) isotope ^{18}F; its radioactivity, difficult handling and very short half-life. For MRI, ^{19}F sensitivity is second only to that of ^{1}H, but, unlike body water detected by ^{1}H MRI, there are no competing ^{19}F background signals.[16] Because ^{19}F MRI signal strength is proportional to the number of equivalent fluorine atoms in a molecule,[17] it is potentially well suited for *in vivo* drug tracking. We previously showed that CA-lys-TFA is a potent *in vitro* substrate for both ASBT and Na+/taurocholate cotransporting polypeptide (NTCP), the key hepatic bile acid uptake transporter.[15] Moreover, CA-lys-TFA demonstrated *in vitro* chemical and enzyme stability and, after oral gavage, concentrated in gallbladders of fasted mice.[15] *In vitro* ^{19}F MRI showed that ^{19}F signals emanating from CA-lys-TFA varied in proportion to its concentration.[15]

The present study was designed to explore the feasibility of using CA-lys-TFA as a probe to assess bile acid transport using *in vivo* ^{19}F MRI. The objective was to compare the *in vivo* imaging performance of CA-lys-TFA with direct measurement of CA-lys-TFA in bile obtained from gallbladders harvested from C57BL/6J wild-type (WT) and Asbt-deficient mice.

EXPERIMENTAL SECTION

CA-lys-TFA Structure and MRI Standard Curve. CA-lys-TFA, a conjugate of trifluoroacetyl L-lysine and the native human primary bile acid cholic acid (Figure 1), was synthesized

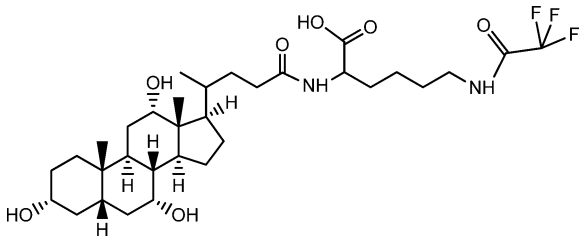

Figure 1. CA-lys-TFA chemical structure. The probe compound is a trifluorinated derivative of cholic acid, formed by conjugating cholic acid to trifluoroacetyl L-lysine.

as described previously.[15] To ensure that a single signal peak was obtained from three equivalent fluorine atoms in CA-lys-TFA, ^{19}F MR spectroscopy was performed. A Varian INOVA 500 MHz NMR machine (Agilent Technologies, Santa Clara, California, USA) was used to analyze CA-lys-TFA in deuterated methanol at 25 °C.

Previously, CA-lys-TFA was imaged *in vitro* using a ^{19}F surface coil.[15] With a surface coil, signal intensity decreases with distance from the coil; this is not the case when using a volume coil. Hence, in the present work, to ensure equivalent ^{19}F signals in the entire anatomical area imaged, a ^{19}F volume coil was used (Bruker Biosciences Corporation, Billerica, Massachusetts, USA). A standard curve was generated by imaging phantoms that consisted of 0, 10, 20, and 30 mM CA-lys-TFA dissolved in methanol in 2 mL glass vials (12 mm diameter, National Scientific, Rockwood, Tennessee, USA).

Animals. All animal experiments were conducted in accordance with the *Guide for the Care and Use of Laboratory Animals* prepared by the U.S. National Academy of Sciences.[18] Both the Institutional Animal Care and Use Committee at the University of Maryland School of Medicine and the Research and Development Committee at the VA Maryland Health Care System approved the mouse experiments. Mice were housed under identical conditions in a pathogen-free environment with a 12:12 h light/dark cycle and free access to standard mouse chow and water prior to treatment.

Two mouse experiments were performed. In the first experiment, 14 mice underwent oral gavage with CA-lys-TFA; 10 mice were subjected to both MRI- and liquid chromatography/tandem mass spectrometry (LC/MS/MS)-based quantification of CA-lys-TFA in the gallbladder. In contrast, mice 11−14 were only evaluated by LC/MS/MS-based quantification. In the second mouse experiment, WT and Asbt-deficient (*Slc10a2*$^{-/-}$) mice underwent gavage with CA-lys-TFA (n = 5 mice per group) and were subjected to either MRI- or LC/MS/MS-based quantification of CA-lys-TFA in the gallbladder.

***In Vivo* Imaging of CA-lys-TFA.** Ten male C57BL/6J mice (average age 9.9 weeks, average weight 24.3 g) were obtained from Jackson Laboratories, Bar Harbor, Maine, USA. Seven mice were fasted overnight and underwent oral gavage with 150 mg/kg CA-lys-TFA in 1:1 polyethylene glycol (PEG) 400:Dulbecco's phosphate buffered saline (DPBS) vehicle. These mice were maintained in the fasted state and imaged either 2 (mice 1−3) or 7 h (mice 4−7) after gavage. Following another overnight fast, mice 2 and 6 were reimaged 48 h after gavage. Mice 8−10 underwent oral gavage with 50 mg/kg CA-lys-TFA in vehicle once daily for 7 days, and were imaged on the seventh day either 2 (mouse 8) or 7 h (mice 9−10) after overnight fasting and final gavage. Previously, we reported that isoflurane, a commonly used anesthetic agent for small-animal MRI, accumulates in the gallbladder in quantities detectable by ^{19}F MRI.[20] Hence, to avoid acquisition of a competing ^{19}F signal isoflurane was not used to anesthetize mice for MRI. Instead, mice were anesthetized with ketamine/xylazine administered via an intraperitoneal (IP) catheter placed before imaging; maintenance doses of ketamine/xylazine were infused every 30 min during imaging. Generally, imaging required 0.5 h for ^{1}H signal acquisition and 1.5 h for ^{19}F signal acquisition, approximately 2 h of MRI for each mouse.

After MRI, mice were euthanized by the injection of additional ketamine/xylazine and exsanguination by intracardiac puncture, and the liver and gallbladder were harvested. CA-lys-TFA concentrations in these organs were determined using LC/MS/MS as described below. Blood was collected in heparinized tubes and centrifuged at 2000g for 15 min, and supernatants were precipitated with four parts acetonitrile. Supernatants were centrifuged at 12000g for 10 min and analyzed by LC/MS/MS. Whole liver and gallbladder were homogenized on ice in a Duall size-21 glass tissue homogenizer

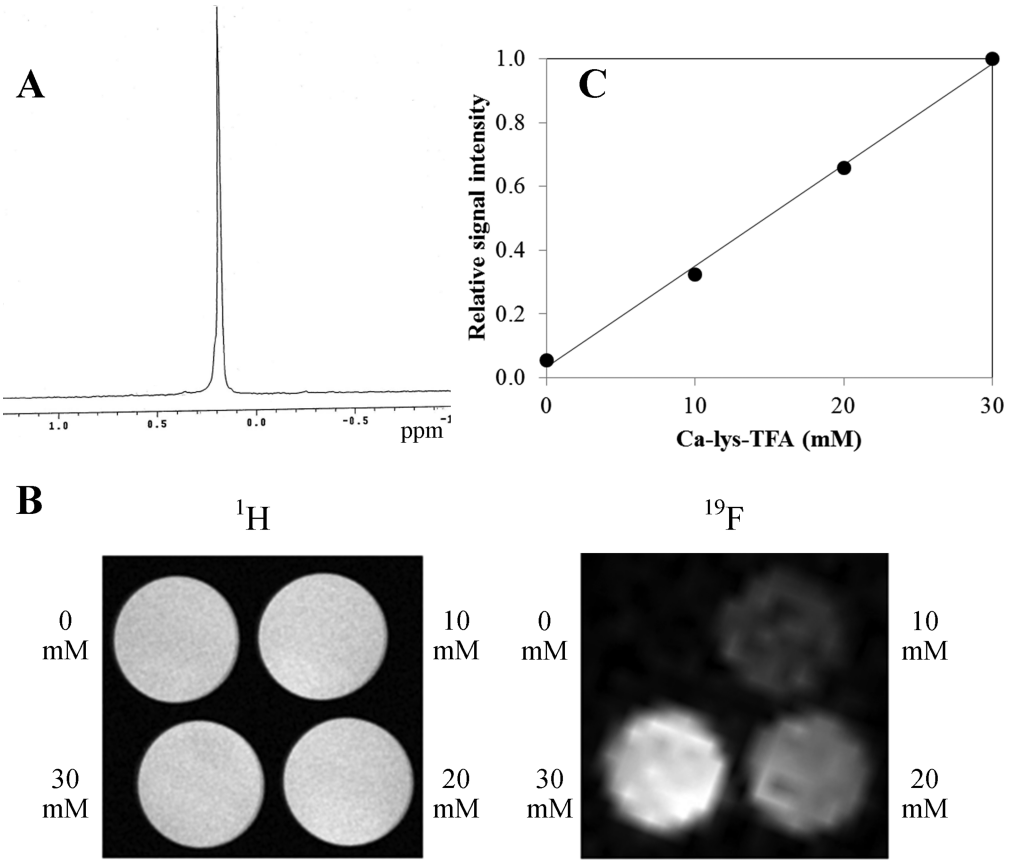

Figure 2. CA-lys-TFA ^{19}F MR spectroscopy and MRI standard curve. (A) ^{19}F MR spectroscopy of CA-lys-TFA in deuterated methanol revealed a single peak for the three equivalent fluorine atoms. (B) ^{1}H (left) and ^{19}F (right) MR images of phantoms containing 0, 10, 20, and 30 mM CA-lys-TFA in methanol. (C) Signal intensity of ^{19}F MR images correlated with CA-lys-TFA concentrations in phantoms. Linear regression yielded R^2 = 0.997.

(Kimble Chase Life Science, Vineland, New Jersey, USA), extracted with 75% acetonitrile and 25% water (800 μL for liver, 300 μL for gallbladder), and centrifuged at 12000*g* for 10 min. Gallbladder extracts were diluted 1000-fold and then quantified by LC/MS/MS.

For mice 8−10, to determine if repetitive 7-day dosing of 50 mg/kg CA-lys-TFA caused tissue injury, sections of liver, stomach, and small intestine were resected and placed in 10% formalin for histological analysis. Unlike single-dose 150 mg/kg CA-lys-TFA,[15] histological examination of relevant abdominal organs had not been performed previously following a repetitive dosing regimen. Tissues were fixed in formalin for three days, transferred to 70% ethanol in water, and stained with hematoxylin and eosin (H&E) for microscopic examination by a senior gastrointestinal pathologist.

To determine if mouse handling after MRI altered gallbladder concentrations of CA-lys-TFA quantified by LC/MS/MS analysis, four additional C57BL/6J male mice were obtained from Jackson Laboratories (mice 11−14, average age 17.4 weeks, average weight 29.6 g) and fasted overnight, and they underwent oral gavage with 150 mg/kg CA-lys-TFA. These mice were maintained in the fasted state and euthanized 8.5 h after gavage without undergoing MRI.

Small Animal MRI. All *in vitro* and *in vivo* ^{1}H and ^{19}F MRI experiments were performed using a Bruker BioSpec 70/30USR Avance III 7T horizontal bore MR scanner (Bruker Biospin MRI GmbH, Germany), equipped with a BGA12S gradient system and interfaced to Bruker Paravision 5.1 for image acquisition and processing. A Bruker 40 mm $^{19}F/^{1}H$ dual-tuned linear volume coil was used to transmit and receive radio frequency (rf) signals at 300.28 MHz for ^{1}H and 282.55 MHz for ^{19}F nuclei. Multislice ^{1}H MR images were acquired using RARE (rapid acquisition with relaxation enhancement) sequence in the cross view of the sample or the body of the animal with repetition time 2200 ms, echo time 8.9 ms, RARE factor 8, field of view 4 × 4 cm^2, slice thickness 1.0 mm, matrix size 266 × 266, in-plane resolution 150 × 150 μm^2, and number of averages 6. Total acquisition time was 7 min and 15 s. ^{19}F images were acquired using a FLASH (fast low angle shot) sequence in the same region of the ^{1}H MRI with repetition time 220 ms, flip angle = 30°, echo time 3.078 ms, matrix size 32 × 32, in-plane resolution 1.25 × 1.25 mm^2, slice thickness 4.0 mm, and number of averages 768. ^{19}F MRI parameters were identical for both calibration phantom images and *in vivo* images with the reference phantom. The flip angle was optimized based on the T1 relaxation time of the phantom. The phantom solvent (methanol) was chosen because of similar signal intensity of CA-lys-TFA dissolved in methanol and human bile (94.2%, Table S1 and Figure S1 in the Supporting Information). Remaining parameters were the same as in the case of ^{1}H MRI. Acquisition time was 1 h and 30 min. Concentrations of CA-lys-TFA in gallbladders were calculated from MR images by determining the mean signal intensity in the gallbladder region of interest (ROI) and comparing this value to the mean signal intensity of the ROI in a phantom placed adjacent to the mouse. In both cases, the ROI was drawn

to exclude the edges of the gallbladder and the phantom, thus avoiding an "edge effect" due to spatial resolution. Reference phantom imaged adjacent to the mouse used 30 mM CA-lys-TFA dissolved in methanol in a short glass NMR tube (5 mm diameter). Mean signal intensity was measured using Paravision 5.1 software. Mouse gallbladder and phantom were simultaneously imaged in the same frame under identical conditions.

Color ^{19}F MR images were obtained using Medical Image Processing, Analysis and Visualization software (MIPAV v7.0.1, CIT, NIH, Bethesda, MD), employing an average image threshold of 0.65, in which the strongest signal (displayed in red) is 1.0. The limit of quantification was assigned to be the noise magnitude plus 2.5 times the noise standard deviation, calculated from an ROI near the periphery of the image. Using this method, there is greater than 99% confidence that voxels containing CA-lys-TFA concentrations above 6.82 mM relative to the phantom are from actual ^{19}F signal, and not noise.[19]

LC/MS/MS. Concentrations of CA-lys-TFA were determined by LC/MS/MS using a Waters Acquity UPLC system with triple quadrupole detector (Waters Corporation, Milford, Massachusetts, USA). The column was a Waters Acquity UPLC ethylene bridged hybrid C8 1.7 μm 2.1 × 50 mm with a flow rate of 0.4 mL/min. The gradient was as follows (expressed as % ACN in water, all mobile phases including 0.1% formic acid): 50% from 0 to 0.5 min, then increased to 95% until 1.5 min, then decreased to 50% at 1.7 min and held at 50% until 2 min. Injection volume was 10 μL. Cone voltage was 75 V, dwell time 0.100 s and collision energy 68 V. Negative electrospray ionization was used with a multiple reaction monitoring method for the transition 631.31 to 241.07 Da. The method was linear over a range of 10 to 2000 nM (R^2 = 0.9998). To measure extraction efficiency, gallbladder extracts (n = 3) were spiked to yield 12 mM CA-lys-TFA and subsequently subjected to sample preparation. The LC/MS/MS determined CA-lys-TFA concentration was 102.5 ± 5.9%.

Asbt knockout mice. Five Asbt-deficient ($Slc10a2^{-/-}$) mice (mice 15−19, average age 42.5 weeks, average weight 28.1 g) and five WT littermates (mice 20−24, average age 44.0 weeks, average weight 28.1 g) were obtained from a colony maintained at the Wake Forest School of Medicine. These mice were fasted overnight and underwent oral gavage with 150 mg/kg CA-lys-TFA. Mice 15−18 and mice 20−23 were maintained in the fasted state and were euthanized without MRI 7 h after dosing, and blood, liver and gallbladder were collected for LC/MS/MS analysis as described above. Mice 19 and 20 were anesthetized with ketamine/xylazine and imaged by MRI as described above.

Data Analysis. Data are presented as average value ± standard error of the mean. Statistical comparisons were performed using the unpaired Student's t test (assuming unequal variance) and were considered significant when two-tailed $P < 0.05$.

RESULTS

Imaging of CA-lys-TFA Phantoms. CA-lys-TFA was detected *in vitro* using both ^{19}F MR spectroscopy (Figure 2A) and MRI with a ^{1}H/^{19}F dual-tuned volume coil (Figure 2B). A single ^{19}F peak resulted from CA-lys-TFA's three equivalent fluorine atoms (Figure 2A). We observed linear relative signal intensity (R^2 = 0.997) for 0, 10, 20, and 30 mM CA-lys-TFA dissolved in methanol in glass vials and imaged concurrently by MRI using a volume coil (Figure 2C).

***In Vivo* Imaging of CA-lys-TFA.** Mice underwent *in vivo* MRI starting approximately 2, 7, or 48 h after oral gavage with a single dose of 150 mg/kg of CA-lys-TFA (mice 1−7) or after 7 days of a daily dose of 50 mg/kg (mice 8−10) (Table 1). Mice were imaged once and euthanized, and blood, liver, and gallbladder were harvested for LC/MS/MS analysis, except mice 2 and 6, which were imaged twice before euthanasia. ^{19}F MRI signals were detected with all dosing regimens and times tested except for the first time mouse 2 was imaged (~2 h after dosing) and the second time mouse 6 was imaged (~48 h after dosing).

Table 1. CA-lys-TFA Gallbladder Concentrations Measured by LC/MS/MS and MRI in Individual Mice[a]

mouse	dose	time of ^{19}F MRI (h)	time of euthanasia (h)	gallbladder wt (mg)	gallbladder [CA-lys-TFA] (mM)	
					LC/MS/MS	MRI
1	150 mg/kg	2.5−4	5.0	24	6.53	14.8
2	150 mg/kg	2.3−3.8	NM	NM	NM	NS
3	150 mg/kg	1.3−1.8	2.8	28	6.73	20.0
4	150 mg/kg	7−8.5	8.6	44	5.48	24.0
5	150 mg/kg	6.9−8.4	8.5	19	4.91	8.6
6	150 mg/kg	6.4−7.9	NM	NM	NM	25.3
7	150 mg/kg	6.8−8.3	8.4	12	1.93	18.1
2	150 mg/kg	49.3−50.8	51.4	23	8.16	24.5
6	150 mg/kg	51.0−52.5	53.0	30	1.45	NS
8	50 mg/kg 7×	1.8−3.3	4.0	14	2.87	10.4
9	50 mg/kg 7×	1.8−3.3	3.5	33	4.46	12.9
10	50 mg/kg 7×	7.3−8.8	8.9	32	3.86	12.3

[a]Each mouse was gavaged with either 150 mg/kg CA-lys-TFA once or repetitively with 50 mg/kg CA-lys-TFA daily for seven consecutive days. Mice 2 and 6, imaged on days 1 and 3 after gavage, lack euthanasia times and LC/MS/MS data for day 1. Times of MRI and euthanasia and gallbladder weights are also recorded. NM = not measured, NS = no detectable signal.

Concentrations of CA-lys-TFA in gallbladders were calculated from MR images by determining the average signal intensity in an ROI within the organ and comparing this value to the average signal intensity detected in an ROI within a 30 mM CA-lys-TFA phantom placed adjacent to the mouse. In nearly all mice, gallbladder CA-lys-TFA concentrations assessed by MRI were lower after repeated dosing with 50 mg/kg than after a single 150 mg/kg dose (Table 1).

Representative MRI images of CA-lys-TFA in gallbladders from mice 1 (Figure 3A) and 4 (Figure 3B), treated with 150 mg/kg CA-lys-TFA and imaged 2 and 7 h after gavage, respectively, demonstrate the ability of this methodology to detect and measure CA-lys-TFA concentrations *in vivo* in the gallbladder. Overlay of images obtained by ^{1}H and ^{19}F MRI signal acquisition indicated clearly that ^{19}F signals emanated from the gallbladder (Figure 3). Also, a more intense ^{19}F signal

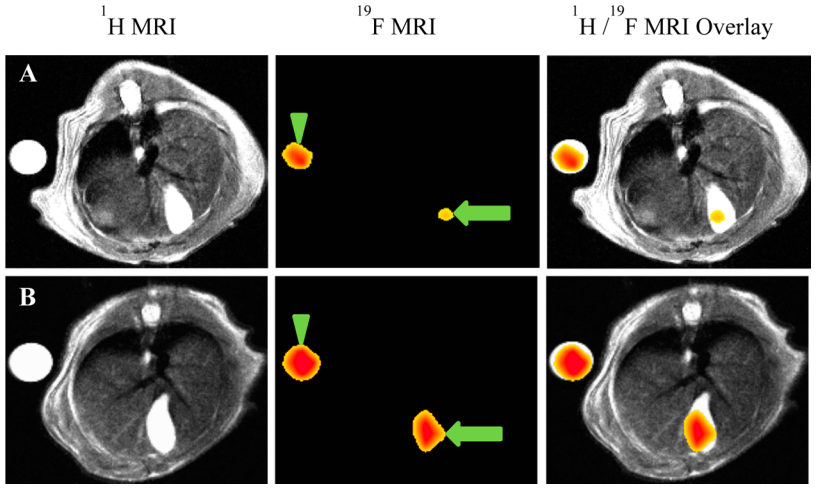

Figure 3. Representative images from two mice imaged after oral gavage with 150 mg/kg CA-lys-TFA. In each image, a 30 mM CA-lys-TFA phantom is adjacent to the mouse. (A, B) Left panels depict abdominal cross-sectional anatomy of the mouse by ^{1}H MRI; the spine is visible at the top and the gallbladder at the bottom. Center panels show ^{19}F MR images obtained from the same cross-sectional area, while right panels show overlays of ^{1}H and ^{19}F images. (A) ^{19}F image acquired ∼2 h after gavage resulted in lower CA-lys-TFA concentration in the gallbladder (arrow) compared to the phantom (arrowhead). (B) ^{19}F image acquired ∼7 h after dosing resulted in similar CA-lys-TFA concentrations in the gallbladder (arrow) and phantom (arrowhead). Of note, individual mice varied in size, e.g., the mouse in panel B was smaller than the mouse in panel A. Hence, the image in panel B "enlarged" the smaller mouse, as well as the phantom. Despite appearances, the mice in panels A and B were not the same size. Likewise, despite appearances, the phantoms were the same size.

was observed at 7 h compared to 2 h (Figure 3). Compared to the MRI signal emanating from the phantom, CA-lys-TFA concentrations in the gallbladder were determined to be 14.8 mM at 2 h (Figure 3A) and 24 mM at 7 h (Figure 3B) (Table 1). Based on these findings, ∼7 h after gavage with CA-lys-TFA was concluded to be the optimal time for ^{19}F MRI, and this time frame and a dose of 150 mg/kg CA-lys-TFA were used for subsequent experiments.

For the 10 mice that underwent MRI and whose gallbladders were subsequently harvested for measurement of CA-lys-TFA levels in gallbladder bile by LC/MS/MS, a correlation was observed between CA-lys-TFA concentrations measured by ^{19}F MRI and corresponding LC/MS/MS (R^2 = 0.54, P = 0.02 for slope parameter). However, as seen in Figure 4A and Table 1, CA-lys-TFA levels calculated from ^{19}F MRI signal intensity in the gallbladder were consistently greater than those measured by LC/MS/MS analysis of gallbladder bile after MRI. We hypothesized that handling mice after MRI (i.e., removal from MRI scanner, transport, and administration of additional sedation before laparotomy and gallbladder harvesting) promoted partial emptying of the gallbladder.

To test this hypothesis, mice 11−14 underwent oral gavage with a single dose of 150 mg/kg CA-lys-TFA and were euthanized 8.5 h later without undergoing MRI. As predicted, in these mice CA-lys-TFA levels measured by LC/MS/MS (average, 11.2 ± 1.7 mM in mice 11−14) were statistically indistinguishable (P = 0.35) from those measured by ^{19}F MRI in other mice at 8.5 h (average, 16.9 ± 4.5 mM in mice 4, 5, and 7). The average CA-lys-TFA concentration measured by LC/MS/MS in gallbladders of imaged mice 4, 5, and 7 was 4.1 ± 1.1 mM, 2.7(±0.8)-fold lower compared to 11.2 ± 1.7 mM in gallbladders from mice 11−14 (P = 0.01). These results could not be explained by differences in gallbladder weights; average gallbladder weights in imaged and nonimaged mice were nearly identical (25 ± 10 vs 23 ± 3 mg, respectively). Overall, these findings supported the hypothesis that post-MRI animal handling reduces gallbladder CA-lys-TFA concentration.

To address these postulated post-MRI animal handling effects, CA-lys-TFA concentrations quantified by ^{19}F MRI and LC/MS/MS (mice 1−10; Table 1) were re-examined and LC/MS/MS concentrations multiplied by a 2.7(±0.8)-correction factor (Figure 4B). Compared to findings when mouse handling after MRI is not considered (Figure 4A), the resultant analysis more closely follows the line of unity for CA-lys-TFA concentrations determined by ^{19}F MRI and LC/MS/MS (Figure 4B). The analysis in Figure 4 was repeated with data at the origin (0,0) excluded and where an intercept was not fitted (Figure S2 in Supporting Information); results of this approach supported the same conclusions. Of note, this 2.7(±0.8)-fold difference may be applicable to the methods here (e.g., Bruker 40 mm ^{19}F/^{1}H dual-tuned linear volume coil) and not to other methods. Additionally, this 2.7(±0.8)-fold difference is a point estimate that assumes an equal post-MRI animal handling effect across all mice.

Bile acids are highly concentrated in the gallbladder. Thus, it was not surprising to find that concentrations of CA-lys-TFA in plasma and liver from mice 1−14 were orders of magnitude lower than those detected in gallbladder (0.70−22.97 μM in liver; 0.02−16.56 μM in plasma vs 1.45−13.93 mM in gallbladder) (Table S1 in Supporting Information): too low to generate ^{19}F MRI signals. Moreover, as we reported previously following a single dose of 150 mg/kg CA-lys-TFA,[15] histological analysis of H&E-stained sections of mouse stomach, liver, and small intestine from mice 8−10 showed no tissue damage after 7-day repetitive dosing with 50 mg/kg CA-lys-TFA. These findings provide reassurance regarding the *in vivo* safety of the novel probe.

Asbt Knockout Mouse Studies. WT mice 15−19 and Asbt-deficient mice 20−24 were gavaged with 150 mg/kg CA-lys-TFA. Mice 15−18 and 20−23 were euthanized 7 h later without MRI. As measured by LC/MS/MS, a striking 30.8-fold difference in the CA-lys-TFA content of gallbladders from WT compared to those from Asbt-deficient mice was observed (9.81 ± 2.13 vs 0.32 ± 0.03 mM, respectively, P = 0.004)

dx.doi.org/10.1021/mp400740c | *Mol. Pharmaceutics* 2014, 11, 1575−1582

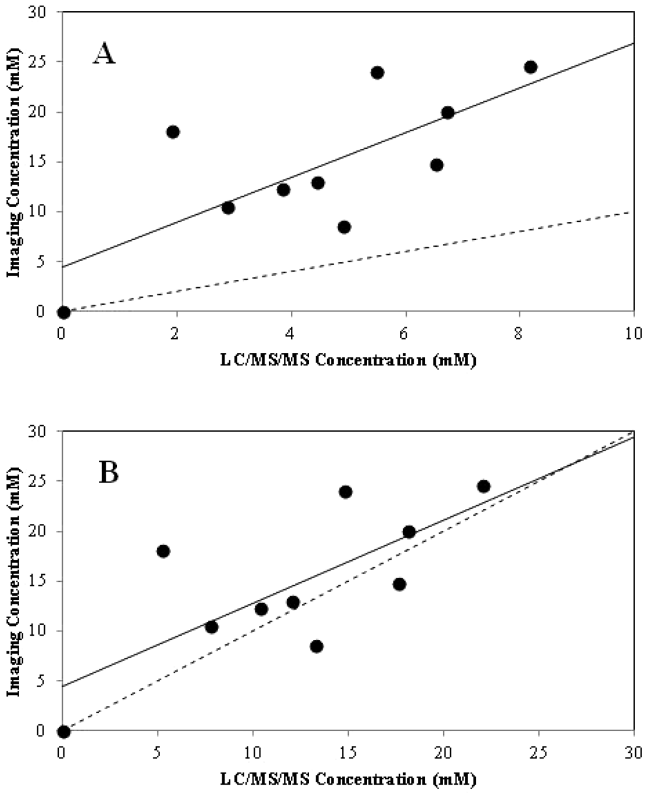

Figure 4. Comparison of gallbladder CA-lys-TFA concentrations calculated from ^{19}F MRI signal intensity to those measured by LC/MS/MS. (A) Calculation of ^{19}F MRI signal intensity in the gallbladders of live, anesthetized mice was accomplished by comparison to the ^{19}F MRI signal intensity of a 30 mM CA-lys-TFA phantom. ^{19}F image acquisition was 1.5 h. CA-lys-TFA content in gallbladder bile by LC/MS/MS was measured after MRI. Each data point represents results from one mouse; MRI-based and LC/MS/MS-based measurements are paired (n = 10 mice). Linear regression analysis (solid line) yielded R^2 = 0.54, P = 0.02, indicating association between MRI-based and LC/MS/MS-determined values. The line of unity is dashed. (B) Comparison of CA-lys-TFA measurements obtained from MRI and LC/MS/MS after applying a 2.7(±0.8) correction factor to LC/MS/MS values to account for a post-MRI effect. The line of unity is dashed, while the line from regression is solid (R^2 = 0.54). The slope from linear regression is 0.83, i.e., 2.7(±0.8)-fold lower than the regressed slope in panel A.

(Figure 5A). These findings predicted that CA-lys-TFA concentrations in gallbladders of Asbt-deficient mice would be below the ^{19}F MRI limits of detection.

To confirm this prediction, mice 19 and 24 were imaged by MRI (^{19}F acquisition time 6.5−8.0 h and 6.6−8.1 h after oral gavage with 150 mg/kg CA-lys-TFA, respectively) and euthanized 9.1 h (mouse 19) and 8.4 h (mouse 24) after gavage. As anticipated, an intense^{19}F gallbladder signal was detected in WT mouse 19 (Figure 5B). CA-lys-TFA measured by LC/MS/MS in gallbladder bile from mouse 19 was 4.81 mM (Table S2 in Supporting Information; equivalent to 13.0 mM after correction for post-MRI animal handling), whereas the concentration measured by MRI was 18.2 mM. In contrast, no ^{19}F signal was detected by MRI in the Asbt-deficient mouse (mouse 24) (Figure 5B). In mouse 24, CA-lys-TFA measured by LC/MS/MS in gallbladder bile was 0.27 mM (Table S2 in Supporting Information; equivalent to 0.73 mM with application of the post-MRI correction factor), confirming that the CA-lys-TFA concentration was indeed below ^{19}F MRI limits of detection. As observed with mice 1−10, CA-lys-TFA levels measured by LC/MS/MS in liver and plasma from mice 15−24 were much lower than those in the gallbladder (Table S2 in Supporting Information), values also well below ^{19}F MRI limits of detection.

■ DISCUSSION

Previously, we showed that the inhaled anesthetic, isoflurane, which like CA-lys-TFA has three equivalent fluorine atoms, can be detected in the gallbladder of live mice using ^{19}F MRI.[20] In the present work CA-lys-TFA, a novel bile acid analogue, was successfully and reproducibly imaged in the murine gallbladder using ^{19}F MRI. To our knowledge, this represents the first report that a drug absorbed orally can be imaged *in vivo* by ^{19}F MRI.

Others have used ^{19}F magnetic resonance spectroscopy (MRS) to detect fluorinated drugs and their metabolites.[21] MRS, however, does not provide spatial information regarding the anatomical location of drugs. Injected or infused drugs, including perfluorocarbons (PFCs) in which all hydrogen atoms in an organic structure were converted to fluorine, have been imaged by ^{19}F MRI. Since fluorine signals can respond to changes in the environment, such as oxygen levels, temperature, and blood flow,[22] PFCs are sometimes used as MRI contrast agents[23,24] or for cell labeling and tracking.[25] In general, PFCs are disadvantaged by low water solubility and thus are not ideal for tagging drugs for oral absorption. Researchers have also taken advantage of high numbers of equivalent fluorine atoms for tagging molecules for use as imaging agents.[17] However, high molecular weight fluorine tags limit drug absorption from the gastrointestinal tract, and large tag size can alter intrinsic activity and disposition compared to the parent molecule.

Visualization of a trifluorinated drug in bile presents a potentially exciting new avenue for imaging the metabolism or biliary excretion of fluorinated drugs. Additionally, the trifluoroacetamidyl group can be used to tag nonfluorinated drugs for imaging, as long as they accumulate spatially in relatively high concentration. Unlike PFCs or compounds with large numbers of equivalent fluorine atoms that were imaged after injection, the trifluoroacetimidyl group was sufficiently small to allow drug absorption from the intestine. In the present work this was achieved by combined passive and active uptake, the latter mediated by the ileal bile acid transporter ASBT.

The ^{19}F MRI limit of detection for CA-lys-TFA in the gallbladder was estimated here to be ∼5 mM as measured by LC/MS/MS after mice were euthanized. The lowest CA-lys-TFA concentration in gallbladder bile detected by LC/MS/MS with corresponding successful detection by MRI was 1.93 mM (corrected value of 5.21 mM) (Table 1, mouse 7), whereas a gallbladder CA-lys-TFA concentration of 1.45 mM (corrected value of 3.92 mM) was not detected by ^{19}F MRI (Table 1, mouse 6 on day 3 after gavage). This limit of detection for ^{19}F MRI by LC/MS/MS (e.g., 5.21 mM) is similar to that directly from ^{19}F MRI (i.e., 6.82 mM), providing further support for the observed 2.7(±0.8)-fold difference. Previously, using a surface coil for ^{19}F MRI, the limit of detection for a trifluorinated drug was estimated to be 1 mM.[20] The current work utilized a volume coil to eliminate signal-to-noise ratio changes that otherwise depend on distance from the coil, and thus allowed the use of a phantom for gallbladder concentration estimation. Of note, limit of detection and signal-to-noise ratio can vary

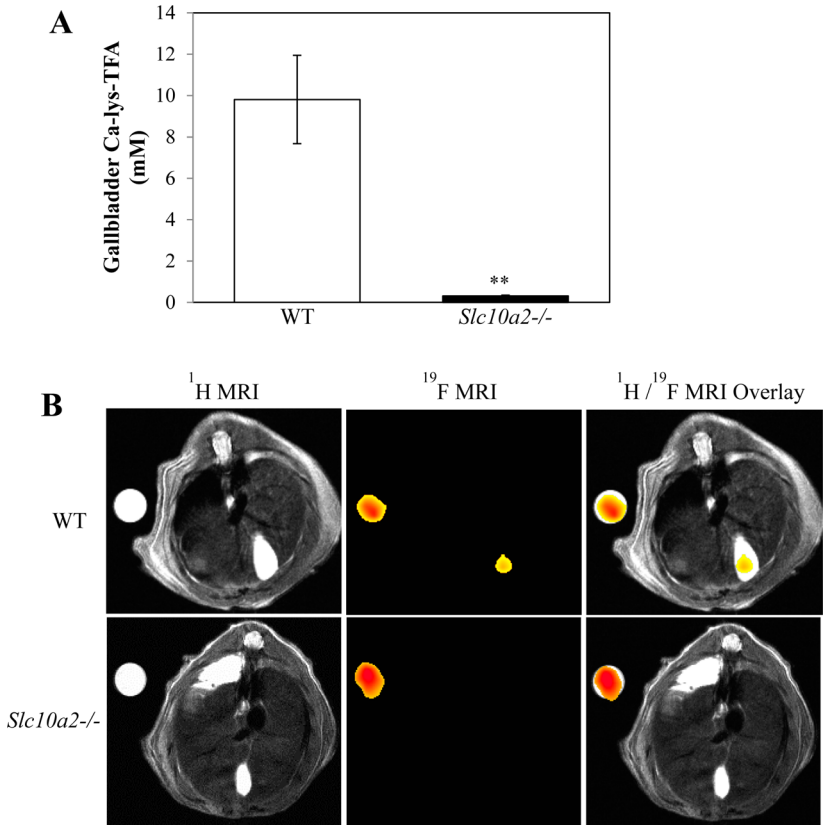

Figure 5. (A) Comparison of gallbladder bile CA-lys-TFA in WT and Asbt-deficient mice. Four WT and four *Slc10a2*−/− mice were gavaged with 150 mg/kg CA-lys-TFA and euthanized 7 h later, and gallbladder bile CA-lys-TFA was measured by LC/MS/MS. CA-lys-TFA was 30.8-fold greater in gallbladders from WT compared to Asbt-deficient mice ($P = 0.004$, Student's *t*-test). (B) Lack of ^{19}F MRI signal for CA-lys-TFA in gallbladder of Asbt-deficient mouse. Images were obtained 6.5−8 h after oral gavage with 150 mg/kg CA-lys-TFA. Left panels show ^{1}H MRI cross-sectional images, center panels show the same cross-sectional images obtained using ^{19}F MRI, and right panels show overlay of ^{1}H and ^{19}F images. MRI of WT mouse shows CA-lys-TFA signal in gallbladder. In contrast, no ^{19}F MRI signal was detected in the Asbt-deficient mouse imaged under the same conditions. ^{19}F MRI acquisition was 1.5 h for both animals.

with imaging acquisition time. Here, a 1.5-h ^{19}F image acquisition time was employed for CA-lys-TFA. In mice, the bile acid pool is ∼4 mg.[26] For a 25-g mouse, the dose was 3.75 mg, which is similar to its pool size. The human bile acid pool is 2−4 g. Thus the detection method has the potential for increased sensitivity or a shorter acquisition time in humans, wherein a much larger gallbladder size would allow for the use of a lower geometric resolution.

A limitation of CA-lys-TFA MRI is the probe's metabolism by gut bacterial enzymes.[15] Bacterial removal of the side chain and hepatic reconjugation with taurine or glycine is part of normal bile acid metabolism and likely accounts for the diminished MRI signal intensity in gallbladder after repetitive dosing with 50 mg/kg daily for 7 days (mice 8−10) and 50 h after dosing with 150 mg/kg (mouse 6) (Table 1).

In mice, Asbt deficiency strikingly reduced gallbladder concentrations of CA-lys-TFA. In WT mice, the average gallbladder bile CA-lys-TFA concentration was 9.81 ± 2.13 mM whereas in Asbt-deficient mice it was 0.32 ± 0.03 mM, a value well below our estimated ^{19}F MRI limit of detection (5 mM). This was confirmed by the absence of a ^{19}F MRI signal in an Asbt-deficient mouse 7 h after gavage with 150 mg/kg CA-lys-TFA, contrasting with the robust signal in a WT mouse (Figure 5). Thus, in this Asbt-deficient mouse model of BAM, ^{19}F MRI following oral dosing with CA-lys-TFA can clearly identify impaired bile acid uptake. Collectively, these findings indicate that CA-lys-TFA, a novel fluorine-labeled imaging agent, has potential as a tool to measure bile acid transport. ^{19}F MR gallbladder imaging, a methodology involving no ionizing radiation, also shows promise as a noninvasive *in vivo* clinical test to diagnose BAM or otherwise impaired bile acid transit.

■ ASSOCIATED CONTENT

Ⓢ Supporting Information

Additional figures for phantom solvent selection and LC/MS/MS vs MRI data analysis and additional tables for phantom solvent selection, liver and plasma CA-lys-TFA concentrations in mice 1−14 and gallbladder, and liver and plasma concentrations of CA-lys-TFA in WT (mice 15−19) and *Slc10a2*$^{-/-}$ mice (20−24). This material is available free of charge via the Internet at http://pubs.acs.org.

■ AUTHOR INFORMATION

Corresponding Authors

*E-mail: jraufman@medicine.umaryland.edu. Phone: 410-328-8728.

*E-mail: jpolli@rx.umaryland.edu. Phone: 410-706-8292.

Present Address

#Division of Pediatric Gastroenterology, Hepatology and Nutrition Emory University School of Medicine, Atlanta, Georgia 30322, United States.

Notes

The authors declare no competing financial interest.

■ ACKNOWLEDGMENTS

We thank Dr. Cinthia B. Drachenberg, Department of Pathology, University of Maryland School of Medicine, for expert histological analysis, and Dr. Bruce Yu, Department of Pharmaceutical Sciences, University of Maryland School of Pharmacy, for helpful discussions. This work was supported by the National Institutes of Health, National Institute of Diabetes and Digestive and Kidney Diseases [Grants DK-093406, DK-067872, DK047987, and DK-081479], National Cancer Institute [Grant CA-120407], and the Food and Drug Administration [Collaborative Agreement U01FD004320].

■ ABBREVIATIONS USED

ASBT, the apical sodium dependent bile acid transporter; BAM, bile acid malabsorption; DPBS, Dulbecco's phosphate buffered saline; FGF, fibroblast growth factor; FLASH, fast low angle shot; H&E, hematoxylin and eosin; IBS, irritable bowel syndrome; IP, intraperitoneal; LC/MS/MS, liquid chromatography/tandem mass spectrometry; MRI, magnetic resonance imaging; MRS, magnetic resonance spectroscopy; NTCP, the Na+/taurocholate cotransporting polypeptide; PEG, polyethylene glycol; PET, positron emission tomography; PFC, perfluorocarbon; RARE, rapid acquisition with relaxation enhancement; rf, radio frequency; ROI, region of interest; WT, wild type

■ REFERENCES

(1) Thomas, C.; Pellicciari, R.; Pruzanski, M.; Auwerx, J.; Schoonjans, K. Targeting bile-acid signalling for metabolic diseases. *Nat. Rev. Drug Discovery* **2008**, *7*, 678−693.

(2) Vallim, T. Q.; Edwards, P. A. Bile acids have the gall to function as hormones. *Cell Metab.* **2009**, *10*, 162−164.

(3) Dawson, P. A.; Haywood, J.; Craddock, A. L.; Wilson, M.; Tietjen, M.; Kluckman, K.; Maeda, N.; Parks, J. S. Targeted deletion of the ileal bile acid transporter eliminates enterohepatic cycling of bile acids in mice. *J. Biol. Chem.* **2003**, *278*, 33920−33927.

(4) Smith, M. J.; Cherian, P.; Ruju, G. S.; Dawson, B. F.; Mahon, S.; Bardhan, K. D. Bile acid malabsorption in persistent diarrhoea. *J. R. Coll. Physicians London* **2000**, *34*, 448−451.

(5) Williams, A. J.; Merrick, M. V.; Eastwood, M. A. Idiopathic bile acid malabsorption—a review of clinical presentation, diagnosis, and response to treatment. *Gut* **1991**, *32*, 1004−1006.

(6) Sciarretta, G.; Fagioli, G.; Furno, A.; Vicini, G.; Cecchetti, L.; Grigolo, B.; Verri, A.; Malaguti, P. 75Se HCAT test in the detection of bile acid malabsorption in functional diarrhoea and its correlation with small bowel transit. *Gut* **1987**, *28*, 970−975.

(7) Wedlake, L.; Thomas, K.; Lalji, A.; Anagnostopoulos, C.; Andreyev, H. J. Effectiveness and tolerability of colesevelam hydrochloride for bile-acid malabsorption in patients with cancer: a retrospective chart review and patient questionnaire. *Clin. Ther.* **2009**, *31*, 2549−2558.

(8) Montagnani, M.; Love, M. W.; Rossel, P.; Dawson, P. A.; Qvist, P. Absence of dysfunctional ileal sodium-bile acid cotransporter gene mutations in patients with adult-onset idiopathic bile acid malabsorption. *Scand. J. Gastroenterol.* **2001**, *36*, 1077−1080.

(9) Oelkers, P.; Kirby, L. C.; Heubi, J. E.; Dawson, P. A. Primary bile acid malabsorption caused by mutations in the ileal sodium-dependent bile acid transporter gene (SCL10A2). *J. Clin. Invest.* **1997**, *99*, 1880−1887.

(10) Walters, J. R.; Tasleem, A. M.; Omer, O. S.; Brydon, W. G.; Dew, T.; le Roux, C. W. A new mechanism for bile acid diarrhea: defective feedback inhibition of bile acid biosynthesis. *Clin. Gastroenterol. Hepatol.* **2009**, *7*, 1189−1194.

(11) Vijayvargiya, P.; Camilleri, M.; Shin, A.; Saenger, A. Methods for diagnosis of bile acid malabsorption in clinical practice. *Clin. Gastroenterol. Hepatol.* **2013**, *11*, 1232−1239.

(12) Pedersen, L.; Arnfred, T.; Thaysen, E. H. Rapid screening of increased bile acid deconjugation and bile acid malabsorption by means of the glycine-l-(14 C) cholylglycine assay. *Scand. J. Gastroenterol.* **1973**, *8*, 665−672.

(13) Merrick, M. V.; Eastwood, M. A.; Anderson, J. R.; Ross, H. M. Enterohepatic circulation in man of a gamma-emitting bile-acid conjugate, 23-Selena-25-Homotaurocholic Acid (SeHCAT). *J. Nucl. Med.* **1981**, *23*, 126−130.

(14) Khalid, U.; Lalji, A.; Stafferton, R.; Andreyev, J. Bile acid malabsorption: a forgotten diagnosis? *Clin. Med.* **2010**, *10*, 124−126.

(15) Vivian, D.; Cheng, K.; Khurana, S.; Xu, S.; Whiterock, V.; Witter, D.; Lentz, K. A.; Santone, K. S.; Raufman, J-P.; Polli, J. E. Design and characterization of a novel fluorinated magnetic resonance imaging agent for functional analysis of bile acid transporter activity. *Pharm. Res.* **2013**, *30*, 1240−1251.

(16) Yu, J. X.; Kodibagkar, V. D.; Cui, W.; Mason, R. P. 19F: A Versatile Reporter for Non-Invasive Physiology and Pharmacology Using Magnetic Resonance. *Curr. Med. Chem.* **2005**, *12*, 819−848.

(17) Jiang, Z. X.; Liu, X.; Jeong, E. K.; Yu, Y. B. Symmetry-guided design and fluorous synthesis of a stable and rapidly excreted imaging tracer for (19)F MRI. *Angew. Chem., Int. Ed.* **2009**, *48*, 4755−4758.

(18) Committee for the Update of the Guide for the Care and Use of Laboratory Animals. National Research Council *Guide for the Care and Use of Laboratory Animals*, 8th ed.; National Academies Press: Washington, DC, 2011.

(19) Srinivas, M.; Morel, P. A.; Ernst, L. A.; Laidlaw, D. H.; Ahrens, E. T. Fluorine-19 MRI for visualization and quantification of cell migration in a diabetes model. *Magn. Reson. Med.* **2007**, *58*, 725−734.

(20) Raufman, J-P.; Xu, S.; Cheng, K.; Khurana, S.; Johnson, D.; Shao, C.; Kane, M.; Shi, D.; Gullapalli, R.; Polli, J. E. *In Vivo* Magnetic Resonance Imaging to Detect Biliary Excretion of 19F-Labeled Drug in Mice. *Drug Metab. Dispos.* **2011**, *39*, 736−739.

(21) Wolf, W.; Presant, C. A.; Waluch, V. ^{19}F-MRS studies of fluorinated drugs in humans. *Adv. Drug Delivery Rev.* **2000**, *41*, 55−74.

(22) Ruiz-Cabello, J.; Barnett, B. P.; Bottomley, P. A.; Bulte, J. W. Fluorine (^{19}F) MRS and MRI in biomedicine. *NMR Biomed.* **2011**, *24*, 114−129.

(23) Flacke, S.; Fischer, S.; Scott, M. J.; Fuhrhop, R. J.; Allen, J. S.; McLean, M.; Winter, P.; Sicard, G. A.; Gaffney, P. J.; Wickline, S. A.; Lanza, G. M. Novel MRI contrast agent for molecular imaging of fibrin: implications for detecting vulnerable plaques. *Circulation* **2001**, *104*, 1280−1285.

(24) Schwarz, R.; Schuurmans, M.; Seelig, J.; Künnecke, B. 19F-MRI of perfluorononane as a novel contrast modality for gastrointestinal imaging. *Magn. Reson. Med.* **1999**, *41*, 80−86.

(25) Janjic, J. M.; Ahrens, E. T. Fluorine-containing nanoemulsions for MRI cell tracking. *Wiley Interdiscip. Rev.: Nanomed. Nanobiotechnol.* **2009**, *1*, 492−501.

(26) Dawson, P. A.; Lan, T.; Rao, A. Bile acid transporters. *J. Lipid Res.* **2009**, *50*, 2340−2357.